Nigerian Journal of Pharmaceutical and Biomedical Research
Vol. 8 Issue.1 April, 2024. p-ISSN: 2579-1419 e-ISSN: 2814-1423

Phytosterols and diterpenoids isolated from *Euphorbia graminea* Jacq. (Asteraceae) leaves exhibit antiproliferative effects against human MCF-7 breast and NCI-H460 lung cancer cell lines

Emmanuel O. Ikpefan [1], Cletus A. Ukwubile [2,*], Edwin O. Omeje [3], Samuel O. Ovbiagele [4], Azhar Mudassar [5], Zadar Ali Shah [6].

[1.] Department of Pharmacognosy and Traditional Medicine, Faculty of Pharmacy, Delta State University Abraka, Nigeria.

[2*] Department of Pharmacognosy, Faculty of Pharmacy, University of Maiduguri, Maiduguri, Nigeria.

[3] Department of Pharmaceutical Chemistry, Faculty of Pharmacy, University of Nigeria Nsukka, 41001, Nsukka, Nigeria.

[4] Ovbioise Hospital, 2 Isibor Agbontaen Street, Aduwawa, Benin City, Edo State, Nigeria.

[5] University of Karachi, International Centre for Chemical and Biological Sciences, Dr Panjwani Center for Molecular Medicine and Drug Research, Karachi, Pakistan.

[6] H.E.J. Research Institute of Chemistry, International Center for Chemical and Biological Sciences, University of Karachi, Karachi-75270, Pakistan.

***Corresponding author:** Email: ile@unimcaukwubaid.edu.ng, doi.org.10.55639/njpbr.1021.002

Abstract

The plant Euphorbia graminea is a tree that has been used in Nigeria for the treatment of various diseases such as cancer, inflammations, diabetes, and ulcers in folk medicine. The present work was aimed at isolating phytosterols and diterpenoids from the leaf extract with potential anticancer and antiproliferative effects against selected cancer cell lines. The chloroform fraction from the 90 % aqueous methanol leaves extract of E. graminea was subjected to vacuum liquid chromatographic fractionation and the fractions were tested at the concentration of 1-100 µg/mL on MCF-7 and NCI-H460 cell lines. Data obtained were statistically analysed using one-way ANOVA followed by Dunnett's post hoc test ($p < 0.05$; $p = 0.001$). The results showed that the chloroform fraction of Euphorbia graminea has demonstrated significant anti-cancer activities against MCF-7 breast and NCI-H460 lung cancer cell lines. Repeated bioassay-chromatographic fractionation of the active fractions yielded four known compounds as triacontan-1-ol, dotriacontan-1-ol, stigmasterol, stigmasta-5-en-3β-ol and a new compound abietane-11, 23 diene-16-oic-14-one whose identities were unequivocally confirmed through detailed NMR and Mass spectroscopic analyses. Against MCF-7 cell lines, dotriacontan-1-ol and abietane-11, 23 diene-16-oic-14-one produced LC_{50} of ~40 and ~91 µM respectively, compared to the ~10 µM produced by standard drug doxorubicin ($p < 0.05$; $p = 0.001$). The LC_{50} against NCI-H460 was observed to be >100 µM for all compounds while doxorubicin gave 15 µM. The isolated compounds from this plant are reported here for the first time. Among the compounds, Dotriacontan-1-ol and Abietane-11, 23 diene-16-oic-14-one were observed to elicit a selective antiproliferative activity on MCF-7 and NCI-H460 respectively hence could be considered as selective natural anticancer agents. However, the mechanism with which these compounds exhibit this activity was not studied and should be considered for future research.

Keywords: **Anticancer, *Euphorbia graminea*, Antiproliferation, SRB assay, Abietane-11, 23 diene-16-oic-14-one.**

Introduction

Plants have a continued history of application in the treatment of cancer (Tavares-Carreón et al., 2020). Although conventional cancer treatments such as radiotherapy and chemotherapy already exist, they have a variety of side effects such as neurological, cardiac, renal, and pulmonary toxicity, which can severely harm a person's health. The growing number have side effects and the high cost of medication has shifted the focus of research toward herbal medicines. As a result, an alternative method for developing anticancer drugs that are less toxic and more potent than those currently available on the market is needed(Onyancha *et al*., 2018).

The prevalence of cancer globally is on the increase ranging from cervical, prostate, lung aetiology, breast, blood, and colon. In terms of etiology, breast cancer is the most common cancer after skin cancer is diagnosed in women worldwide. Men and women can be diagnosed with breast cancer, but it is most common in women. On the other hand, lung cancer affects the lungs, especially in people who smoke. The non-small cell lung cancer is the most prevalent of all lung cancers with about 85 % of cases globally (Abuzaid, *et al*,2020). Cancers remain one of the diseases that have little or no cure globally because, various treatment measures such as chemotherapy, radiotherapy, and surgery have yielded little or no solution at all. In Nigeria, various medicinal plants have been used and are continuously used to manage and treat various types of cancers. These ethnobotanical prescriptions in Nigeria's traditional medicine have produced great success in cancer therapy, and one such plant used is *Euphorbia graminea* Jacq. which was confirmed from the world flora online (Ikpefan *et al*., 2020).

The plant *Euphorbia graminea* is commonly called the grass leaf spurge and was previously known as *Agaloma graminea* (Ikpefan et al., 2023) belongs to the class of untapped plant species. It has been reported as an invasive species which is native to northern Mexico and Peru (Dilleniaceae *et al*., 2022). Apart from its native origin, it has been reported to have spread to other parts of the world such as Taiwan, Galapagos Islands and Nigeria (Tchimene *et al*., 2016). The plant is morphologically made up of tiny, glanduliform stipules, petaloid gland appendages and leaves with entire margin (Aigbokhan & Ekutu, 2015). It has been reported to have leaves that are alternate below and opposite above and have apex which ranges from acuminate to acute, bases which are acute to obtuse surfaces which are pubescent and shapes which are ovate-rounded to oblong.

In Nigeria and other parts of the world, there is little or no information documented on the phytochemistry and biological activities of *E. graminea*. However, traditional healers in some parts of the world such as Columbia have reported the use of the plant in the treatment of numerous diseases such as skin infections, ulcers, warts, and cancer (Tchimene et al., 2016). It has also been reported to be poisonous to ruminants (Dilleniaceae et al., 2022). In Nigeria, there are no existing reports on the phytochemical contents of this plant, despite the uses of this plant for treating various disease conditions.

Previous research on this plant showed that the chloroform fraction outperformed the aqueous fraction and the methanol extract in terms of antiproliferative activity (Antiproliferative et al., 2021). This current research was aimed at isolating, characterize and elucidate structurally antiproliferative phytosterols and diterpenoids from chloroform fraction of *E. graminea* and

study their effects on MCF-7 breast and NCI-H460 lung cancer cell lines.

Materials and Methods

Collection of plant materials

The fresh leaves of *E. graminea* was collected in the evening hours at a location within the University of Benin campus, Nigeria. Authentication of the plant was made by a taxonomist Mr. Adewale of the International Institute for Forest Research, Ibadan, Nigeria. A voucher specimen number of FHI 109024 was deposited for the plant. The leaves were then dried under-shade for two weeks, reduced into fine powder using milling machine and stored for further use.

Extraction and purification of bioactive fraction of extract

A total of 2.5 kg of the powdered leaves of *E. graminea* were exhaustively extracted by applying a Soxhlet apparatus using 95 % aqueous methanol (5.5 L) as the extracting solvent. The extract was dried *in vacuo* at 40 ^{0}C and was subjected to exhaustive solvent-solvent partitioning using chloroform and 70 mL distilled water. A portion of the active chloroform fraction (98.50 g) previously obtained from the extract (200 g) as earlier reported (State et al., 2023), was subjected to standard vacuum liquid chromatography on normal-phase silica gel using C_6H_{14} (100 %), C_6H_{14}-CH_2Cl_2(1:1; 1:3), CH_2Cl_2 (100 %),$CHCl_2$-$CH_3COOC_2H_5$ (3:1,1:1,1:3), $CH_3COOC_2H_5$(100%), $CH_3COOC_2H_5$–CH_3OH(1:1) and CH_3OH (100 %) (1.5 L) in increasing polarity, to afford ten (10) fractions which were concentrated *in vacuo* at 45 ^{0}C .Analytical thin layer chromatographic analyses of the Vacuum Liquid Chromatographic fractions of the chloroform fraction was carried out on a pre-coated aluminium plate of Silica gel GF_{254} using DCM: CH_3OH (9.4: 0.6). After development, the plates were sprayed with ceric sulphate spray and subsequently heated for 5 min at 110°C (Ukwubile *et a*l., 2019). The coloured spots were noted and their R_f values were recorded. Based on observations made on the results obtained, coupled with the TLC profile, the chloroform VLC sub-fraction of *E. graminea* were bulked into CA (1-4), 5-9(CB) and 10(CC) accompanied by biological test at concentration between 1-100 µg/mL.

Silica gel column chromatography purification of sub-fraction

Column chromatographic purification of sub-fraction CB (5-9/74.56g) using silica gel (60-120 mesh) and mobile phases using 800 mL of *n*-hexane (100%), *n*-hexane-ethyl acetate (99: 1, 97:3, 95:5,93:7,90:10,80:20, 70:30, 50:50), $CH_3COOC_2H_5$ (100%), $CH_3COOC_2H_5$-CH_3OH (90:10, 80:20, 50:50) and CH_3OH (100%) further resulted in one hundred and twelve (112) fractions which were bulked into seven sub-fractions (1-2, 3-6, 7-12, 13-14, 15-18, 19-24, 25-112) after thin layer chromatographic analysis using *n*-hexane-ethyl acetate (3:2) solvent system. All fractions were screened at a single concentration of 75 µg/mL. Fractions13-14, 15-18 and 19-24 precipitated out and were purified by washing with DCM and Hexane (HPLC grade solvents) and the resulting pure compounds were coded as EGC13, EGC15 and EGC19. Sub-fractions 25-112 [116.202mg] were re-chromatographed using reverse phase chromatographic analysis on C_{18}-reversed phase silica gel (40-63 µm) and was eluted with 300 mL of 100 % H_2O, H_2O:CH_3OH (70:30, 60:40, 50:50, 40: 60, 30:70, 20:80, and 10:90) and 100 % CH_3OH to give 13 fractions (RC1-RC13) were subjected to biological activities using MCF-7 and NCI-H460 cell lines at a

single concentration of 50 µg/mL. Sub-fractions RC-13 (68.55mg) re-chromatographed by preparative TLC analyses on 0.5 mm Silica gel G_{F254} using n-hexane-ethyl acetate (3:2) and developed three times. Using UV at 254 and 356nm, four bands were scrapped, eluted, concentrated and coded as S-1, S-1^1, S-2 and S-2^1. Isolate compounds S-1, $S1^1$ and S2, $S2^1$ were combined and coded as S1and S2 respectively whose purity were confirmed by TLC analyses using chloroform-methanol (3:2) and n-hexane-ethyl acetate (3:2) as solvent systems (Ukwubile *et al*., 2019)

Characterization and structure elucidation of isolated compounds

The structures of the isolated compounds were determined using MS, 1D and 2D NMR (^{1}H/ ^{1}H COSY, NOESY; ^{1}H/ ^{13}C HSQC and HMBC) spectroscopic analysis carried out on a Bruker Avance DRX spectrometer at 500 MHz (1H) or 125 MHz (13C), with $CDCl_3$ as solvent. Two-dimensional experiments (^{1}H/ ^{1}H COSY, NOESY; ^{1}H/ ^{13}C HSQC and HMBC) were set up and processed with standard Bruker software. The signals of the deuterated solvent were taken as reference (Hurlimann, n.d.).

SRB antiproliferative assay

The cells (MCF-7 and NCI-H460) were cultured with 10% FBS, 1% l-glutamine and antibiotic solutions (penicillin-streptomycin-amphotericin) supplemented with DMEM (Dulbecco's Adapted Eagle's Medium). The SRB assay method by Mbaoji *et al*. (Akah et al., 2012) and Nguyen et al. (Bessède et al., 2014), were adopted with slight modifications. Briefly, cells (10000 cells/well/100 µL were seeded for confluence formation and incubated in CO_2 incubator at 37 ºC for 24 h. The anti-proliferative activities of fractions (1-100 µg/mL) and isolated compounds (1-100 µM) were carried out on breast (MCF-7) and lung (NCI-H460) cancer cell lines using the sulforhodamine-B assay. The various concentrations of the fractions (1-100 µg/mL) and isolated compound (1-100 µM) were added (100 µL/well) in appropriate wells and incubated for 48 h. Appropriate controls and blanks (drug and extract) were prepared. At the end of 48 h, time zero-1 (T_{z1} plate) and time zero-2 (T_{z2} plate) plates were fixed with gentle addition of 50 % w/v cold TCA (50 µL/well) before and after the addition of the test samples in experimental plates. These were left at room temperature for 30 min, washed (3x) and dried overnight. After 48 h, experimental plates were also fixed. The dried fixed plates were stained with 100 µL of sulforhodamine solution (0.4 % wt/vol prepared in 1 % acetic acid) for 10 min followed by washing (5x) with 1 % acetic acid to remove excess stain and air-dried. Finally, 100 µL of tris base solution (pH 10.2, 10 mM) was added and absorbance was recorded at 545 nm using a micro-plate reader. The results of the extracts, fractions and compounds were presented as GI_{50} (growth inhibition of 50 % of cell population), TGI (total growth inhibition) and LC_{50} (lethal/killing concentration for 50 % of cell population) and expressed in µg/mL (Pillai *et al*., 2022).

Statistical analysis

All data were expressed as mean ± SD (n=3). The values of $p < 0.05$ were considered statistically significance using one-way analysis of variance (one-way ANOVA) followed by Dunnett's post hoc test as was analyzed using GraphPad Prism version 9 (UK).

Results

The results in Table 1 showed that the bulked VLC sub-fractions (CA-CC) of *E. graminea* on MCF-7 and NCI-H460 cell lines at concentrations between 1-100 µg/mL showed fraction CB (5-9) was the most active as it

produced cytotoxicity of 1.26 and 3.89 % at 75 and 100 µg/mL respectively. At similar concentrations, CA (1-4) and CC (10) produced growth inhibitions of 84.53, 94.40 and 41.55 and 58.60 % respectively. LC_{50} for the three fractions were observed to be greater than 100 µg/mL while fraction CB (5-9) had TGI and GI_{50} of 76 and 23 µg/mL (Table 1).

Table 1. Effects of the VLC fractions of *E. graminea* on MCF-7 cell lines

Bulked VLC Fractions	Conc. (µg/mL)	(%) Growth Inhibition/cytotoxicity	GI_{50}	LC_{50}	TGI
			(µg/mL)		
CA(1-4)	1.0	0.00 ± 0.00	97.82± 2.0*	>100	>100
	25	+30.53 ± 2.94			
	50	+54.08 ± 2.94			
	75	+84.53 ± 1.53			
	100	+94.40 ± 1.0			
CB (5-9)	1.0	+12.50 ± 0.04	22.72± 0.0*	>100	76±0*
	25	+66.08 ± 1.31			
	50	+80.10± 1.01			
	75	–1.26 ± 0.07			
	100	–3.89 ± 0.29			
CC (10)	1.0	0.00 ± 0.00	>100	>100	>100
	25	0.00 ± 0.00			
	50	+12.22± 0.14			
	75	+41.55 ± 0.19			
	100	+58.60 ± 0.25			

- sign represents cytotoxicity, + sign represents growth inhibition. GI_{50} = growth inhibition of 50% of cell population, TGI = total growth inhibition, and LC_{50} = lethal/killing concentration for 50% of cell population. Column chromatographic fractionation of CB gave 112 fractions bulked into C1-C6. While fractions C4 (13-14) and C5 (15-24) precipitated and were cleaned up and coded as EGC13 and EGC15 respectively, fraction C6 (25-112) was subjected to reverse phase chromatographic analysis yielding 94 sub-fractions bulked into RCI-RC10 bulked fractions with RC10 showing activity against the cell lines (RCI-RC9 were inactive). *Statistically significant at $p < 0.05$ (one-way ANOVA followed by Dunnett's post hoc; $P = 0.001$).

In addition, the trend of activity on NCI-H460 was also like that of MCF-7 but there was no cytotoxic effect even at the maximum concentration of 100 µg/mL. At 75 and 100 µg/mL, CA produced 29.65 and 61.67 % growth inhibition while CB gave 81.26 and 89.85 % respectively against NCI-H460. However, CC was observed to be inactive at 100 µg/mL. Both the TGI and LC_{50} were greater than 100 µg/mL for all the fractions. Hence, fractions CB (5-9) was the most active and was selected for further purification (Table 2).

Table 2. Effects of the bulked VLC fractions of *E. graminea* on NCI-H460 Cell

VLC fractions	Conc. (µg/mL)	(%) Growth Inhibition	GI_{50}	LC_{50}	TGI
			(µg/mL)		
CA(1-4)	1.0	0.00± 0.00	92 ± 4*	>100	>100
	25	0.00 ± 0.00			
	50	+14.20 ± 0.42			
	75	+29.65 ± 1.46			
	100	+61.67 ± 8.07			
CB(5-9)	1.0	+19.73 ± 0.06	54 ± 0.05*	>100	>100
	25	+53.57 ± 2.55			
	50	+67.54± 1.22			
	75	+81.26 ± 4.84			
	100	+89.85 ± 1.21			
CC(10)	100	<50	>100	>100	>100

GI_{50} = growth inhibition of 50% of cell population, TGI = total growth inhibition, and LC_{50} = lethal/killing concentration for 50% of cell population. *Statistically significant at $p < 0.05$ (one-way ANOVA followed by Dunnett's post hoc; P = 0.001).

The antiproliferative studies of the subsequent chromatographic sub-fractions (C1-C6) from CB (5-6), at single concentration of 75 µg/mL showed higher antiproliferative activities on both cell lines as they recorded cytotoxicity of -73. 00 and -61.0 % as well as -13.52 and -11.18 % on MCF-7 an NCI-H460 cell lines, respectively (Plate 1). Antiproliferative activities of the bulked reversed phase column chromatographic fractions at a single concentration of 50 µg/mL against MCF-7 breast and NCI-H460 lung cell lines showed RC10 produced cytotoxicity of 22.95 and 9.30 %, respectively which resulted in cytotoxic effects of the compounds against the cell lines and subsequent prevention of metastasis (Plate 1). However, sub-fractions RC1-RC9 were recorded to be inactive on both cell lines with their GI_{50}, LC_{50} and TGI >50. Fractions RC10 were subjected to preparative thin layer chromatographic analysis and two compounds S1 and S2 were isolated. At 75 and 100 µM, compound EGC 19 (Plate 1; Table 3) and S2 were observed to produce growth inhibitory effects of 54, 78, 80 and 91 %, respectively against MCF-7 cell lines with GI_{50} of 62 and 54 µM.

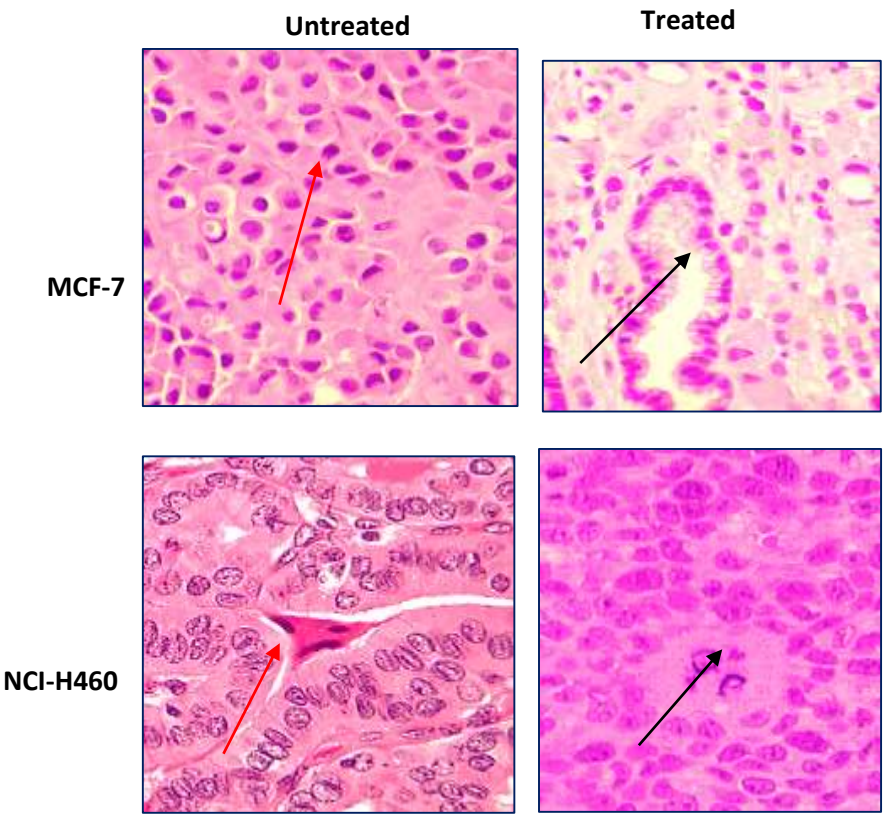

Plate 1. Photomicrographs of cancer cells exposed to various concentrations of Abietane-11, 23 diene-16-oic-14-one. The red arrows indicate live cancer cells and black arrows indicate apoptotic cells, 40x.

EGC 13

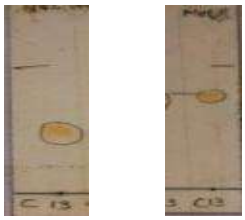

1 2

Plates	Solvent system	RF
1	C_6H_{14} :$CH_3COOC_2H_5$ (9.2 : 0.8)	0.46
2	CH_2Cl_2: CH_3OH (9.8 : 0.2)	0.67

EGC 15

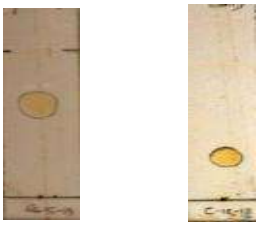

1 2

Plates	Solvent system	RF
1	CH_2Cl_2: CH_3OH (9.8 : 0.2)	0.58
2	C_6H_{14} :$CH_3COOC_2H_5$ (9.9 : 0.1)	0.34

EGC 19

1

2

Plates	Solvent systems	R_F
1	C_6H_{14}: $CH_3COOC_2H_5$ (9 1)	0.42
2	CH_2Cl_2:CH_3OH (9.8 0.2)	0.56

S1

1

2

3

Plates	Solvent system	R_f
1	C_6H_{14} :$CH_3COOC_2H_5$ (9.2 : 0.8)	0.88

S2

1

2

3

Plates	Solvent system	R_f
1	C_6H_{14} :$CH_3COOC_2H_5$ (9.2 : 0.8)	0.52

Plate 2. Chromatograms showing compounds EGC13, EGC15, EGC19, S1 and S2 from the column chromatographic analysis of the bioactive fraction of *E. graminea.* Adsorbent- Silica gel (C_6H_{14}:$CH_3COOC_2H_5$ (9.8:0.2; 9:1). Spray reagent- Ceric acid sulphate, heated at 110°C.

At the same concentrations, while compound EGC 19 recorded GI_{50}, LC_{50} and TGI's of 19.4,40.5 and 32.6 µM, S1 was observed to produce GI_{50}, LC_{50}, TGI of 34, 91.4 and 56.27±8.23µM respectively (Table 3). The higher activity of EGC15 (Plate 2) and S1 was similarly observed against NCI-H460 cell lines with the former and latter having GI_{50} and TGI of 50 and 89 µM and 63 and 94 µM respectively. However, they were observed to produce LC_{50} higher than 100 µM (Plate 2; Tables 3 and 4). These cytotoxic effects displayed by these compounds were statistically significant ($p<0.05$) when compared to doxorubicin standard drug.

Table 3. Growth Inhibitory and Cytotoxic Effect of the isolated compounds on MCF-7 Cell Lines

Compound	Conc. (µM)	% Growth Inhibition/ cytotoxicity	GI_{50}	LC_{50}	TGI
			(µM)		
EGC 13	100	<50	>100	>100	>100
EGC15	1.0 25 50 75 100	+14 ± 2.51 +54 ± 3.80 –65 ± 5.33 –73 ± 3.70 –93 ± 3.14	19.4 ± 0.33*	40.5 ± 0.21*	32.60±5.01
EGC19	1.0 25 50 75 100	0.00 ± 0.00 0.00 ± 0.00 +18.00 ± 1.81 +54.98 ± 7.80 +78.00± 3.17	62.40± 0.12*	>100	>100
S1	1.0 25 50 75 100	+3.50 ± 1.00 +14.90 ± 2.00 +63.00 ± 18.00 +84.60 ± 8.00 – 4.30 ± 1.40	33.65 ± 0.74*	91.40±6.95*	>100
S2	1.0 25 50 75 100	+13 ± 1.55 +28 ± 2.17 +46 ± 0.75 +80 ± 1.45 +91 ± 1.61	53.90 ± 5.85*	>100	>100
Doxorubicin	0.01 0.1 0.5 5.0 10.0	+4 .00± 1.0.00 +37.00 ± 5.00 +81.00 ± 2.00 –18.00 ± 3.00 –70.00 ± 2.00	0.55 ± 0.08*	10±0.2*	11 ± 1.0*

- sign represents cytotoxicity, + sign represent growth inhibition, GI_{50} = growth inhibition of 50% of cell population, TGI = total growth inhibition, and LC_{50} = lethal/killing concentration for 50% of cell population. *Statistically significant at $p < 0.05$ (one-way ANOVA followed by Dunnett's post hoc; P = 0.001).

Table 4. Growth Inhibitory/Cytotoxic Effect of EGC 13, EGC15 and EGC -19 on NCI-H460 Cell Lines

Compound	Conc. (μM)	% Growth Inhibition/ cytotoxicity	GI_{50}	LC_{50}	TGI
			(μM)		
EGC 13	100	<50	>100	>100	>100
EGC15	1.0	+0.00 ± 0.00	50.00 ± 11.50*	>100	88.84±7.68*
	25	+19.30 ± 1.08			
	50	+51.00 ± 3.36			
	75	+94.00 ± 5.95			
	100	–17.20 ± 8.72			
EGC19	100	<50	>100	>100	>100
S1	1.0	+0.00 ± 0.00	62.9 ±5.11*	>100	94.2 ±14.01*
	25	+8.02 ± 0.98			
	50	+41.00 ± 8.60			
	75	+68.13 ± 5.80			
	100	–1.79 ± 0.68			
S2	1.0	+0.00 ± 0.00	86.4 ±7.50*	>100	>100
	25	+0.00 ± 0.00			
	50	+12.30 ± 4.48			
	75	+48.98 ± 7.80			
	100	+66.00 ± 3.17			
Doxorubicin	0.01	+1.00± 0.10	1.98 ± 0.10*	14.7± 1.0*	16.1± 3.10*
	0.1	+4.00 ± 2.00			
	0.5	+52.00 ± 18.00			
	5.0	–12.00 ±6.00			
	10.0	–58.00 ± 3.50			

*Statistically significant at $p < 0.05$ (one-way ANOVA followed by Dunnett's post hoc; $P = 0.001$).

The compound EGC 13 (Triacontan-1-ol) was isolated as a pale white solid (Plate 2). The ^{1}HNMR spectrum (Fig. 1) recorded at 600 MHz showed a 3-proton triplet at δ 3.26 and 0.84 were allotted the CH_3 end chain. By using the ^{13}C NMR spectrum at 150 MHz (Fig. 2), the compound was further structurally elucidated. At 76.60 ppm was a signal for carbon connected to primary alcohol group (R-OH) (Rosandy et al., 2013). The methylene protons (CH_2) showed downfield signals at chemical shifts of 14.10, 25.70, 29.30, and 31.90 ppm. From the spectra, the isolated compound was analyzed to be $C_{30}H_{62}O$. In addition, the presence of various fragmentation patterns having 14 and 28 atomic mass unit variations as

well as lack of aligning peaks to $[M-15]^+$ revealed the aliphatic nature of the isolated compound (Fyad et al., 2020). From the revelations mentioned above, it can be confirmed that the compound was a saturated long chain compound belonging to the alcohol group triacontane-1-ol which is a known compound (Hurlimann, n.d.). This compound has been reported to have pharmacological properties which include, anti-inflammatory, antimicrobials and antioxidants (Lalthanpuii & Lalchhandama, 2020).

Compound EGC 15 (dotriacontan-1-ol) (Plate 2) which is like triacontan-1-ol but differs by C_2H_4 ethylene group, was isolated as a pale white powder. The ^{1}HNMR spectral (500 MHz; $CDCl_3$) in Figure 1 at chemical shift 0.86 ppm revealed six methyl protons which are triplets. A clear signal at δ 1.25 with integration of 64 protons that the compound contained 32 CH_3 groups in a nearly similar chemical environment. In the ^{13}C NMR spectrum (Fig. 6) recorded at 125 MHz, the signals were observed only at δ 14.11, 23.00, 25.74, 29.40, 29.70, 31.93 and 32.83. The peak at δ 63.12 was interpreted to be carbon atom connected to the OH group. The peaks at chemical shift 14.11, 23.00, 25.74, 31.93 and 32.83 ppm revealed the presence of the CH_3 group in the compound which showed the aliphatic nature of the compound. Because of these reasons we concluded that the compound was a long chain OH hydrogen-carbon-containing compound; dotriacontan-1-ol (Fyad et al., 2020). This compound is like EGC 13 (Plate 2) earlier described in that they are both long chain aliphatic fatty acid, but EGC 15 differs in having two additional ethylene molecules (C_2H_4). Previously reported data on the compound corresponds with ours (Lynch et al., 2023).

EGC19 (β-Sitosterol) was isolated as white powder (21 mg). All other spectral data of compound EGC19 were unambiguously like those of Stigmasterol except that it showed a saturated side chain and has only one double bonds of olefinic protons in the cyclohexane ring. Thus, one olefinic proton doublet (Fig.1) signal at δ 5.35 ppm was related to the carbon signal at δ 121.72 ppm an indication that the compound is likely β-Sitosterol. The observed pseudo ^{13}C-NMR signals (Fig. 2) at 138.33 and 129.25 ppm are attributable to minute impurities of stigmasterol, which usually remain incompletely resolved except for critical purification steps. EGC19 was unambiguously characterized as β- Sitosterol based on perfect agreement of present spectral data with previously reported literature data for sitosterol (20). Previous studies have reported β-Sitosterol to reduce the inhibitory effect on carcinogen-induced cancer of the colon (Jiang et al., 2017).

The structure of the compound was further affirmed with the aid of 2D spectral data including HSQC, HMBC and NOESY NMR (Fig.3). Compound S2 (β-stigmasterol) was isolated as a white powder with a melting point of 261.25 ^{o}C. The compound tested positive to the usual Lieberman Burchard steroidal nucleus test. The positive mode electron impact ionization (EI^+) mass spectral data of this compound gave a mass, m/z 413.4 (M^+) corresponding to the molecular formula $C_{29}H_{48}O$. The ^{1}H-NMR spectral (Fig. 1) data of compound S2 had three olefinic methine proton signals of two double bonds at δ 5.33, 5.15, and 5.00 ppm and they were related to four olefinic carbon signals at δ 121.71, 129.28, 138.31, and 140.76 ppm with the cyclic quaternary carbon signal at 140.76 ppm disappearing in the DEPT-135 and DEPT-90 spectra for the compound. Furthermore, ^{1}H-NMR data showed

the typical C-3 proton resonating as multiplets at 3.51 ppm confirming the usual oxygenated C-3 of steroids (Torres et al., 2014). In all, the ^{13}CNMR (Fig. 2), clearly showed presence of 29 carbon atoms made of 6 methyl, 9 methylene, 11 methines and 3 quaternary carbons. Altogether, the above data strongly suggested that compound S2 is β-Stigmasterol and agrees with existing literature data for Stigmasterol (Lalthanpuii & Lalchhandama, 2020). The structure of the compound was further affirmed with the aid of 2-D spectral data including NOESY (SM. 4), HSQC and HMBC measurements. On the other hand, Compound S1 was isolated as a white powder, mp 305.43 °C and showed negative Liebermann-Burchard test. The spectra information obtained showed S1 could be a new compound (Tables 5 and 6).

For compound S1, the positive mode electron impact ionization (EI^+) and GCMS (Fig. 4) showed an m/z of 413.4 corresponding to a mass of 412.4 g/mole, corresponding to a molecular formula of $C_{27}H_{40}O_3$. This can be seen in the spectra data of compound S1(Tables 5 and 6). The compound exhibited an ABX spin system in ^{1}H-NMR spectrum (Fig. 1) typical of the Abietane diterpenoid nucleus (Abuzaid et al., 2020). The ^{13}C-NMR (Fig. 2) showed presence of two carbonyl functional groups and a total of twenty-seven carbons made of up of 6 methyl, 6 methylene, 10 methines and 5 quaternary carbons. The HMBC correlation (Tables 5 and 6) confirmed presence of the typical isopropyl side chain with an olefinic carbon and strongly correlated with C15. The compound appeared to be isolated as a combination of two isomers comprising Δ 11, 12; Δ 23, 24 and Δ 6, 7; Δ 23, 24 forms. However, the Δ 11, 12; Δ 23, 24 was in higher proportion as could be inferred from the proton NMR spectrum. The spectral features of Compound S1 were typical of an Abietane diterpenoid but have not been reported in literature as having been isolated from natural source including the current source, *E. graminea*. Taking together, the compound S1 was unequivocally characterized as Abietane-11, 23 diene-16-oic-14-one to be known commonly as ‘’Ikpefbietane’’. Most plants of the genus *Euphorbia* have been reported to contain abietane diterpenoids, which usually have an extra α, β-unsaturated γ-lactone ring located between C-12 and C-13 and some of which have an epoxy ring at C-8 and C-14, or C-11 and C-12. Many of these abietane diterpenoids have also been reported to exhibit inhibitive activity on various types of tumor cells, such as ANA-1, B16 Jurkat cells (22), K562 cells and LNCaP cells (Abduh, 2023).

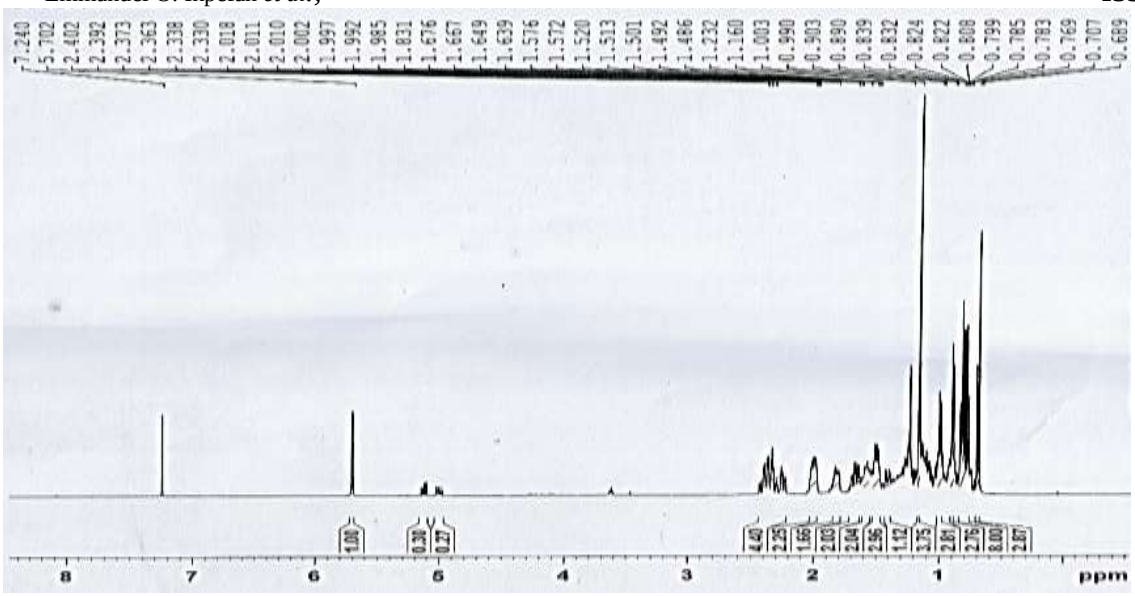

Fig. 1. [1]H-NMR spectrum of compound S1 (Abietane-11, 23 diene-16-oic-14-one).

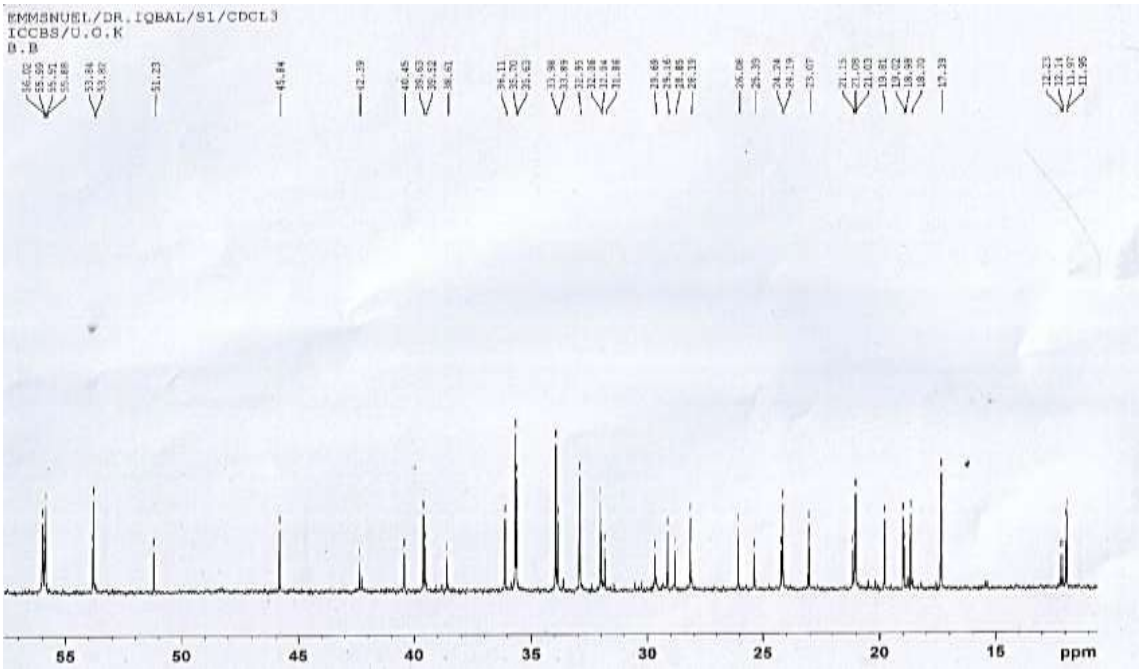

Fig. 2. [13] C-NMR (B.B) of compound S1 (Abietane-11, 23 diene-16-oic-14-one).

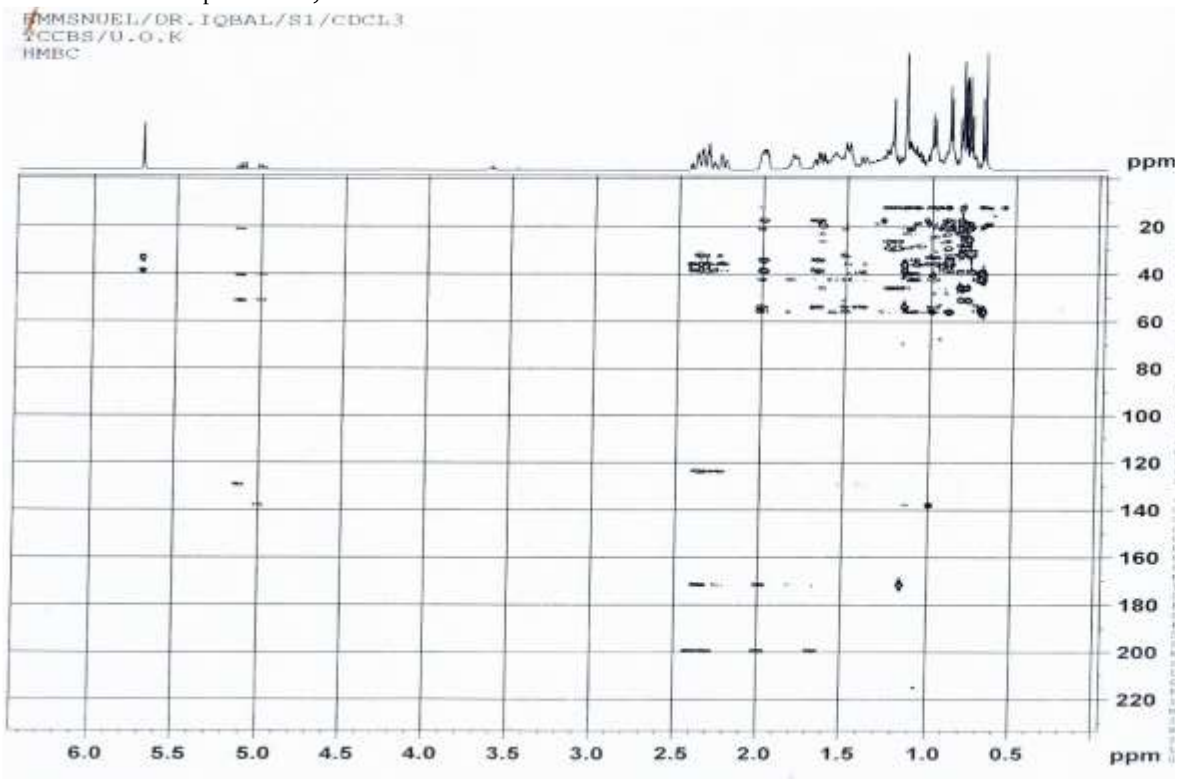

Fig. 3. [13] HMBC of compound S1 (Abietane-11, 23 diene-16-oic-14-one).

Table 5. Spectral data of the Abietane Diterpenoid (Δ 11, 12)

S/No	^{1}H-NMR (500 MHz, $CDCl_3$)	13C-NMR Carbon	DEPT	HMBC
1	2.35, m	33.9	CH_2	C2, C3, C10, C17
2	1.4-1.5, m	21.2	CH_2	C1, C3, C4, C10
3	1.16, m	39.6	CH_2	C1, C2, C4, C5
4	-	38.6	-	C5, C18, C19
5	1.07, m	55.8	CH	C6, C7, C10
6	1.18, m	26.1	CH_2	C5, C7, C8
7	0.98, m	24.2	CH_2	C6, C8, C9
8	0.90, d	53.8	CH	C7, C9, C14
9	1.00, d	56.0	CH	
10	-	42.4	-	
11	5.70, s	123.7	CH	C9, C13
12	-	123.7	-	C13, C14, C15
13	0.92, d	45.8	CH	C14, C14, C16
14	-	199.8	-	
15	1.51, m	40.5	CH	C13, C20
16	-	177.7	-	
17	0.89, d	18.7	CH_3	C1, C10
18	0.80, d	21.2	CH_3	C3, C4, C5, C19
19	0.83, m	21.1	CH_3	C3, C4, C5, C18
20	2.01, m	36.1	CH	C15, C21, C22
21	1.4, dd	25.4	CH_2	C20, C22

22	1.16, s	17.4	CH_3	C20, C21	
23	5.15, dd	138.1	CH	C15, C20, C24	
24	5.00, dd	129.5	CH	C20, C23, C25	
25	1.50, m	51.2	CH	C24, C26, C27	
26	0.82, d	12.0	CH_3	C24, C25, C27	
27	0.70, d	12.2	CH_3	C24, C25, C26	

Table 6. Spectral data of the Abietane Diterpenoid (Δ 6, 7)

S/No	^{1}H-NMR (500 MHz, $CDCl_3$)	13C-NMR Carbon	DEPT	HMBC
1	2.35, m	33.9	CH_2	C2, C3, C10, C17
2	1.4-1.5, m	21.2	CH_2	C1, C3, C4, C10
3	1.16, m	39.6	CH_2	C1, C2, C4, C5
4	-	38.6	-	C5, C18, C19
5	1.07, m	55.8	CH	C6, C7, C10
6	5.70, s	123.7	CH	C5, C7, C8
7	5.70, s	123.7	CH	C5, C6, C8, C14
8	0.90, d	53.8	CH	C7, C9, C14
9	1.00, d	56.0	CH	
10	-	42.4	-	
11	1.18, m	26.1	CH_2	C5, C7, C8
12	3.52, m	76.5	-	C13, C14, C15
13	0.92, d	45.8	CH	C14, C14, C16
14	-	199.8	-	
15	1.51, m	40.5	CH	C13, C20
16	-	177.7	-	
17	0.89, d	18.7	CH_3	C1, C10
18	0.80, d	21.2	CH_3	C3, C4, C5, C19
19	0.83, m	21.1	CH_3	C3, C4, C5, C18
20	2.01, m	36.1	CH	C15, C21, C22
21	1.4, dd	25.4	CH_2	C20, C22
22	1.16, s	17.4	CH_3	C20, C21
23	5.15, dd	138.1	CH	C15, C20, C24
24	5.00, dd	129.5	CH	C20, C23, C25
25	1.50, m	51.2	CH	C24, C26, C27
26	0.82, d	12.0	CH_3	C24, C25, C27
27	0.70, d	12.2	CH_3	C24, C25, C26

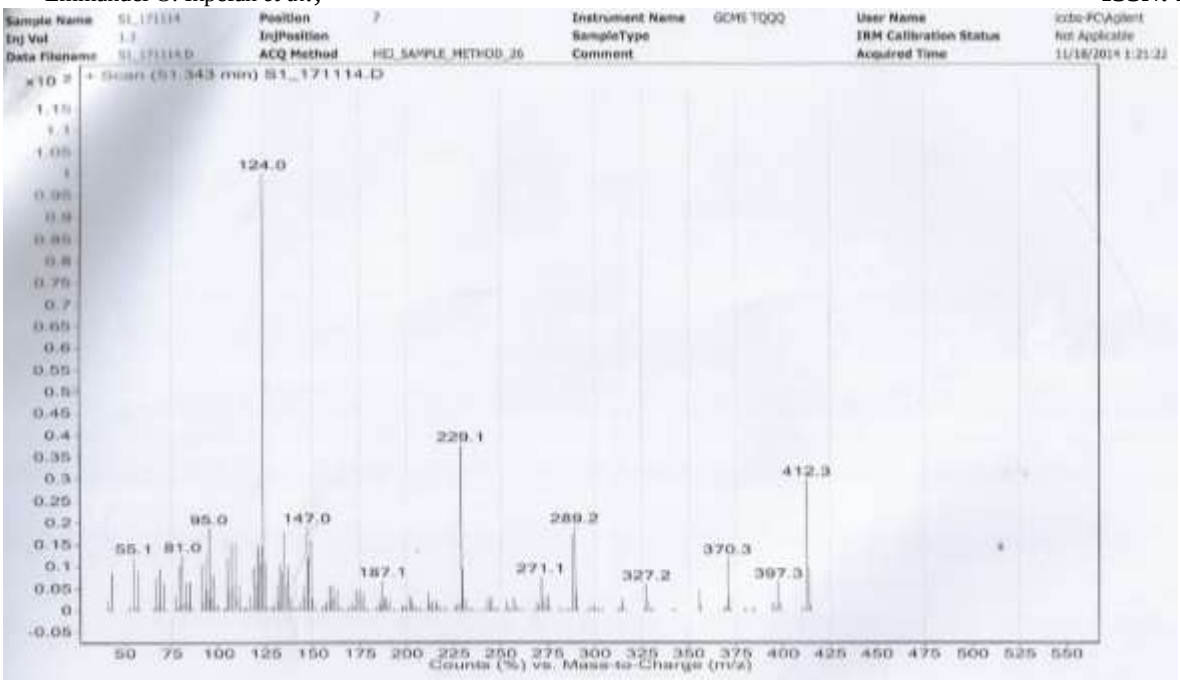

Fig. 4. Mass spectra sheet (GCMS) of sample S1 (of Abietane-11, 23 diene-16-oic-14-one)

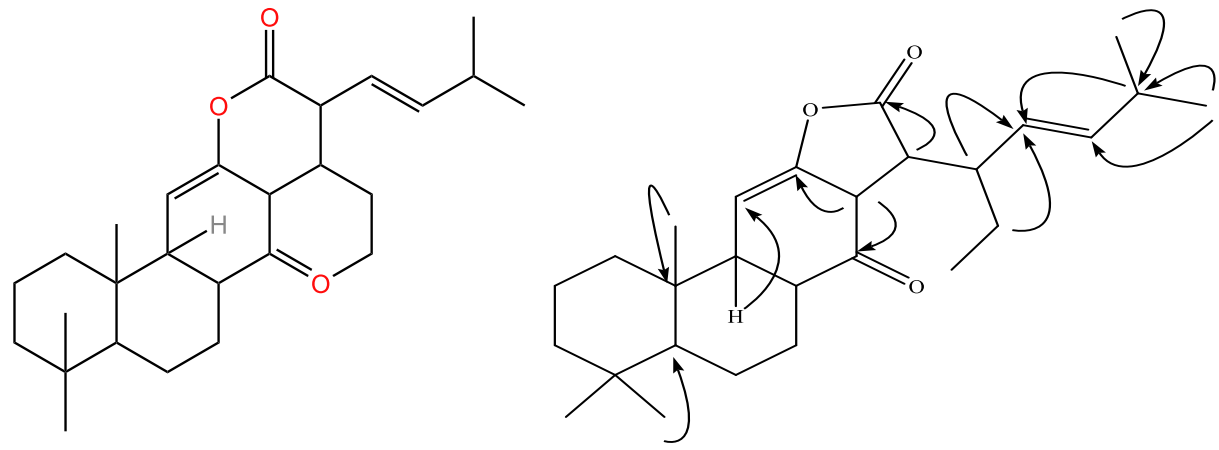

a. b.

Fig. 5. Proposed structure (a) and configuration (b) of S1 (Abietane-11, 23 diene-16-oic-14-one).

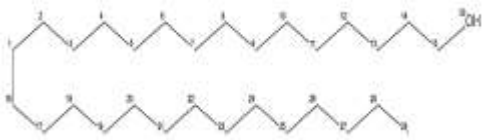

EGC 13

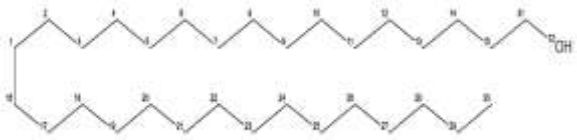

EGC 15

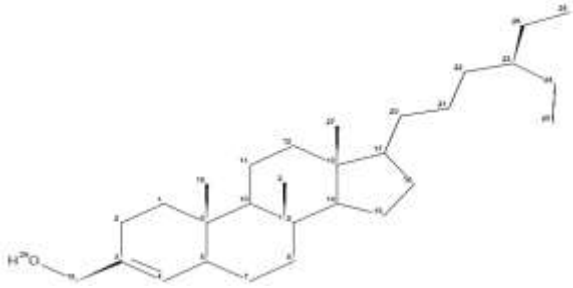

EGC 19

S2

Fig. 6. Proposed structures of other compounds (1-4) isolated from *E. graminea.*

Discussion

From the current study, unlike compound S1, compounds EGC 13 (Triacontan-1-ol), EGC 15 (Dotriacontan-1-ol), EGC 19 (β-sitosterol) and S2 (β-stigmasterol) had spectra data similar to already existing compounds isolated from plants (Lalthanpuii & Lalchhandama, 2020). The TLC was used to check the purity of isolated compounds by obtaining a single spot of the plate (Plate 2).

Unlike the breast cancer cell lines (MCF-7) (Plate 1), the effects of the fractions against lung cancer cells (NCI-H460) were observed to be growth inhibitory rather than cytotoxic effects. Lung cancers have been reported to be the most difficult form of cancer to treat (Tavares-Carreón et al., 2020). This may explain why the fractions and compounds only retarded the growth and not cytotoxic. Relating the activities of compound EGC 19 (β-Sitosterol), S1 (Abietane-11, 23 diene-16-oic-14-one) (Tables 5 and 6) and S2 (β-Stigmasterol) revealed some variation in their biological activities. These variations could be due to the extra α, β-unsaturated γ-lactone ring in S1 and double bonds in S2. The aim of the present study at isolating the anti-proliferative bioactive constituents from the chloroform fraction of *E. graminea* was achieved. This was due to the fact that a total four known compounds comprising of two fatty alcohols (Triacontan-1-ol and Dotriacontan-1-ol) and two stigmastane (β-sitosterol and β-stigmasterol) (Lalthanpuii & Lalchhandama, 2020), as well as a new diterpene (Abietane-11,

23 diene-16-oic-14-one l) were isolated and their structures were elucidated via spectroscopic methods. The most important data were gained from NMR measurements. 1D and 2D NMR (^{1}H NMR and ^{13}C NMR) spectra were recorded for all the compounds. To the best of our knowledge, these compounds were isolated for the first time from this plant. The anticancer mechanism of these diterpenoids and phytosterols are not fully understood but is believed that they induce apoptosis in cancer cells by controlling the signal pathway of PI3K/Akt as well as production of mitochondrial-derived reactive oxygen species (mROS), while their growth inhibitory effects are majorly dependent on the modulatory effect against cyclin proteins and cyclin-dependent kinase (Porter & Jänicke, 1999) .

Our study showed the presence of five bioactive compounds from chloroform fraction of *E. graminea* leave extract. The isolated compounds including the new Abietane-11, 23 diene-16-oic-14-one was isolated from this plant for the first time, and they were observed to exhibit a selective antiproliferative effects against the cell lines as they were more active on MC-7 compared to NCI-H460 cell lines. The results of this study show that *E. graminea* can significantly inhibit the growth of human MCF-7 and NCI-H460 cells and contains a contains a new compound, Abietane-11, 23 diene-16-oic-14-one, whose novelty requires further investigation The results suggest that Abietane-11, 23 diene-16-oic-14-one is viable and this compound offers a new avenue for chemotherapeutic intervention after it has been clinically investigated. The study further affirms the use of *E. graminea* extract for the treatment and management of cancers in Nigeria.

Acknowledgements

The authors are grateful to Cancer Research Laboratories especially those in Pakistan for technical assistance helps.

Conflicts of interest

We have none to declare.

References

Abduh, M. S. (2023). *Anticancer analysis of CD44 targeted Cyclosporine loaded thiolated chitosan nanoformulations for sustained release in triple-negative breast cancer*. https://doi.org/10.2147/IJN.S424932

Abuzaid, H., Amin, E., Moawad, A., Usama Ramadan, Abdelmohsen, Hetta, M., & Mohammed1, R. (2020). Liquid Chromatography High-Resolution Mass Spectrometry Analysis, Phytochemical and Biological Study of Two Aizoaceae Plants Plants: A New Kaempferol Derivative from Trianthema portulacastrum L. *Pharmacognosy Research*, *10*(October), 24–30. https://doi.org/10.4103/pr.pr

Aigbokhan, E. I., & Ekutu, O. (2015). Aspects of the biology and ecology of Euphorbia graminea Jacq . (Euphorbiaceae) – a potentially invasive herbaceous plant in Nigeria. *Nigerian Journal of Botany*, *25*(1), 35–53.

Akah, P. A., Nworu, C. S., & Mbaoji, F. N. (2012). *Genus Detarium : Ethnomedicinal , phytochemical and pharmacological profile*. *3*(2), 367–375.

Antiproliferative, I. N. V., Of, A. A., Extract, T. H. E., Fractions, P., & Leaves, O. F. (2021). In Vitro Antiproliferative And Antioxidant Assessment Of The Extract And Partitioned Fractions Of Leaves Of Euphorbia Graminea Jacq. (Euphorbiaceae). *Nigerian Journal of Pharmacy*, *55*(2), 26–31.

https://doi.org/10.51412/psnnjp.2021.5

Bessède, E., Staedel, C., Acuña Amador, L. A., Nguyen, P. H., Chambonnier, L., Hatakeyama, M., Belleannée, G., Mégraud, F., & Varon, C. (2014). Helicobacter pylori generates cells with cancer stem cell properties via epithelial-mesenchymal transition-like changes. *Oncogene*, *33*(32), 4123–4131. https://doi.org/10.1038/onc.2013.380

Dilleniaceae, L., Sidiq, L. O., Nkumah, A. O., Oyinloye, B., & Ogbole, O. O. (2022). *Evaluation of Antioxidant and Antimicrobial Activities of Euphorbia graminea L . (Euphorbiaceae) and Tetracera scandens*. *10*, 123–128.

Ikpefan, E. O., Enwa F. O. and Emebrado, O. (2020). Euphorbia graminea Jacq. (Euphorbiaceae): The antimicrobial assessment of the extract and fractions of the leaves. *Nigerian Journal of Pure and Applied Sciences*, *33*(2), 3809–3818. https://doi.org/10.48198/njpas/20.b15

Fyad, K., Belboukhari, N., Hadj-Khelil, A. O. El, & Sekkoum, K. (2020). Analgesic and anti-inflammatory activity of aqueous extract of Bubonium graveolens. *Biomedical Research and Therapy*, *7*(9), 4002–4009. https://doi.org/10.15419/bmrat.v7i9.632

Hurlimann, M. D. (n.d.). *Introduction to NMR spectroscopy NMR : the background*.

Ikpefan, E. O., Ikpefan, J. O., Ovbiagele, S. O., Ejienyafu, U., & Ojumah, C. B. (2023). Euphorbia Graminea Jacq. (Euphorbiaceae): A Comparative Antimicrobial Evaluations of Stem and Root Extracts. *Journal of Applied Sciences and Environmental Management*, *27*(2), 249–255. https://doi.org/10.4314/jasem.v27i2.10

Jiang, L., Wang, W., He, Q., Wu, Y., Lu, Z., Sun, J., Liu, Z., Shao, Y., & Wang, A. (2017). Oleic acid induces apoptosis and autophagy in the treatment of Tongue Squamous cell carcinomas. *Scientific Reports*, *7*(1), 1–11. https://doi.org/10.1038/s41598-017-11842-5

Lalthanpuii, P. B., & Lalchhandama, K. (2020). Phytochemical analysis and in vitro anthelmintic activity of Imperata cylindrica underground parts. *BMC Complementary Medicine and Therapies*, *20*(1), 1–9. https://doi.org/10.1186/s12906-020-03125-w

Lynch, H. N., Authement, C. C., Maczko, A., Parker, M., Beaty, K., & Liyana Pathiranage, A. (2023). Gas Chromatography-Mass Spectrometry Analysis of Cannabis: Undergraduate Organic Chemistry Laboratory Exercise. *Journal of Chemical Education*, *100*(3), 1303–1312. https://doi.org/10.1021/acs.jchemed.2c00966

Onyancha, J. M., Gikonyo, N. K., Wachira, S. W., Mwitari, P. G., & Gicheru, M. M. (2018). Anticancer activities and safety evaluation of selected Kenyan plant extracts against breast cancer cell lines. *Journal of Pharmacognosy and Phytotherapy*, *10*(2), 21–26. https://doi.org/10.5897/jpp2017.0465

Pillai, J. R., Wali, A. F., Menezes, G. A., Rehman, M. U., Wani, T. A., Arafah, A., Zargar, S., & Mir, T. M. (2022). Chemical Composition Analysis, Cytotoxic, Antimicrobial and Antioxidant Activities of Physalis angulata L.: A Comparative Study of Leaves and Fruit. *Molecules*, *27*(5). https://doi.org/10.3390/molecules27051480

Porter, A. G., & Jänicke, R. U. (1999). Emerging roles of caspase-3 in apoptosis. *Cell Death and Differentiation*, *6*(2), 99–104. https://doi.org/10.1038/sj.cdd.4400476

Rosandy, A. R., Din, L. B., Yaacob, W. A., Yusoff, N. I., Sahidin, I., Latip, J., Nataqain, S., & Noor, N. M. (2013). Isolation and characterization of compounds from the stem bark of Uvaria rufa (Annonaceae) | Pemisahan dan

Pencirian sebatian dari Kulit batang Uvaria rufa (Annonaceae). *Malaysian Journal of Analytical Sciences*, *17*(1), 50–58.

State, O., Biology, C., State, D., & Akporhuarho, A. (2023). *GC-MS* Characterized Bioactive Constituents and Antioxidant Capacities Of Aqueous And Ethanolic Leaf Extracts of Rauvolfia Vomitoria : A Comparative Study. 21(2), 479–499.

Tavares-Carreón, F., De La Torre-Zavala, S., Arocha-Garza, H. F., Souza, V., Galán-Wong, L. J., & Avilés-Arnaut, H. (2020). In vitro anticancer activity of methanolic extract of Granulocystopsis sp., a microalgae from an oligotrophic oasis in the Chihuahuan desert. *PeerJ*, *2020*(3), 1–21. https://doi.org/10.7717/peerj.8686

Tchimene, M. K., Okoli, C. O., & Iwu, M. M. (2016). *Antidiabetic property of some Nigerian medicinal plants*. *10*(11), 139–148. https://doi.org/10.5897/JMPR2015.5895

Torres, R., Manalo, C., Zinca, R., Walde, M., & Garbo, A. (2014). Characterization of the Leaf Extract of Annona muricata and Larvicidal Activity against Aedes aegypti. *Time Journals of Biological Sciences and Technology*, *2*(3), 33–40. www.timejournals.org/tjbst

Ukwubile, C. A., Ahmed, A., Katsayal, U. A., Ya'u, J., & Mejida, S. (2019). GC–MS analysis of bioactive compounds from Melastomastrum capitatum (Vahl)Fern. leaf methanol extract: An anticancer plant. *Scientific African*, *3*, 10–17. https://doi.org/10.1016/j.sciaf.2019.e00059